Calibration of the model in simplified (under Co^{++}) conditions

The calibration of the Müller cell (MC) model was performed to determine the optimal combination of electrical parameters (R_o, R_i, and R_m) and input resistance (R_{inp}) that produced the best fit between the experimental and computational data. It required intensive calculations (including more than 90% of all simulations in this work) and carries an important supportive function.

A sample of the light-induced $[K^+]_o$ changes at different retinal depths and the simultaneously recorded intraretinal electrical responses of the mouse retina which was superfused with Ames solution containing Co^{++} are shown in Fig. S3.1. Since this work is focused on MCs, the records distal to 85% of the retinal depth are omitted.

In this experiment Co^{++} suppressed all post-receptoral activity, both electrical and ionic. As a result, only the PIII component of the ERG remained. It consists of two subcomponents – fast PIII (fPIII) and slow PIII (sPIII). The fPIII is generated by the photoreceptors and it is clearly visible in the ONL (64 – 85% of retinal depth) as a faster increase in potential than at more proximal depths. In these layers it overlaps with the MC-generated sPIII, but only sPIII is present at more proximal depths.

The $[K^+]_o$ decrease is a result of the light-induced hyperpolarization of the photoreceptors, and it originates in the photoreceptor layer. But these K^+ changes propagate, somewhat surprisingly, all over the retina, partly by diffusion and partly through MCs by spatial buffering mechanisms. Thus, the MC's membrane experiences the hyperpolarizing effect of decreasing $[K^+]_o$ along the whole length of the cell. But the hyperpolarization in the distal parts of the MC is larger than in the proximal part because the distal K^+ changes are bigger than the proximal ones. This difference in local membrane potentials manifests extracellularly as sPIII.

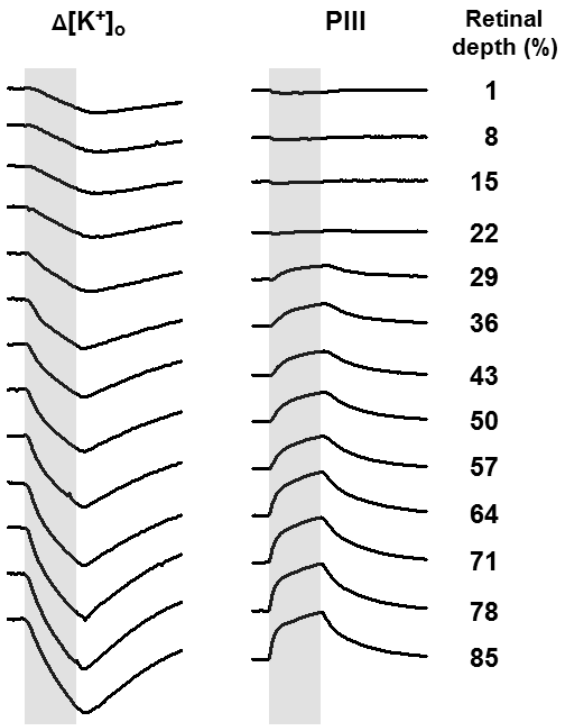

Fig. S3.1. Depth profiles of light-induced $\Delta[K^+]_o$ and PIII responses in the retina treated with 2mM Co^{++}. The retinal depth (in %) is measured from zero at the vitreal (grounded) surface of the retina. The grey area marks the light stimulus (3 s in duration). For the amplitude scaling, the space between the start of $\Delta[K^+]_o$ traces is 0.5 mM, and the space between the start of PIII traces is 2 mV.

Based on the K^+ measurements presented in Fig. S3.1, a detailed 3-D matrix of light-induced $[K^+]_o$ changes in the Co^{++}-treated retina was created. The matrix consists of 8100 values of $[K^+]_o$ organized in 81 rows, one per each % of the retinal depth, and 100 columns, one per 0.1 s of time starting 1 s before the light onset; it is visualized as a 3-D color map surface (Fig. S3.2A) and as the color-filled contour plot (Fig. S3.2B). The custom-made program accepted the matrix of $[K^+]_o$ as an input and calculated transretinal potentials generated by the MC using the model described in the Methods. The comparison of these computed potentials with the real potentials measured at three critical retinal depths - 29 % (distal part of IPL), 43 % (middle of INL), and 57% (OPL,

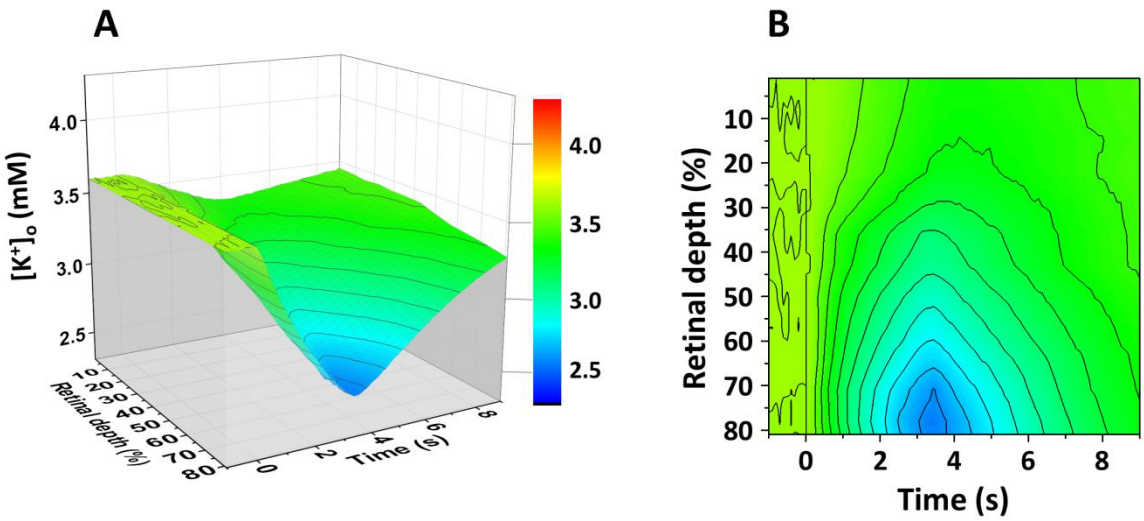

Fig. S3.2. Light-induced $[K^+]_o$ changes in the mouse retina treated with Co^{++}. *A*. The 3-D color map surface. *B*. The color-filled contour plot. Time = 0 corresponds to the start of the light stimulus that lasts for 3 s.

near the border with ONL) - is presented in Fig. S3.3. Black lines are the experimentally measured voltages, and red lines are the simulations calculated for the corresponding depth. Different distributions of R_o, R_i and R_m were used for calculations in each group. A combination of sets o1 (for R_o) and i1 (for R_i) were used for simulations presented in the upper row of the figure (parts A, B, and C) and sets o2 and i2 were used for simulations in the lower row (parts D, E, and F). These were combined with one of three distributions of R_m in different columns of the figure: set m1 for parts A and D, set m2 for parts B and E, and set m3 for parts C and F. It should be remembered that in the case of R_m the sets determined only relative values; the absolute value depends on the selected input resistance (R_{inp}) of the cell. With R_o and R_i chosen and fixed, the larger R_{inp}, the smaller the extracellular potentials. Thus, to find the best fit between experimental and computed potentials different R_{inp} values were tested (with a precision of 1 MΩ). Unsurprisingly, the optimal R_{inp} varied depending on combinations of R_o, R_i, and R_m settings, but its values (from 25 to 33 MΩ for the calculations presented in Fig. 7) lay well within the range

suggested for the mouse MC by the literature (from 14.7 MΩ (Newman, 1987) to 90.5 MΩ (Reichelt *et al.*, 1993).

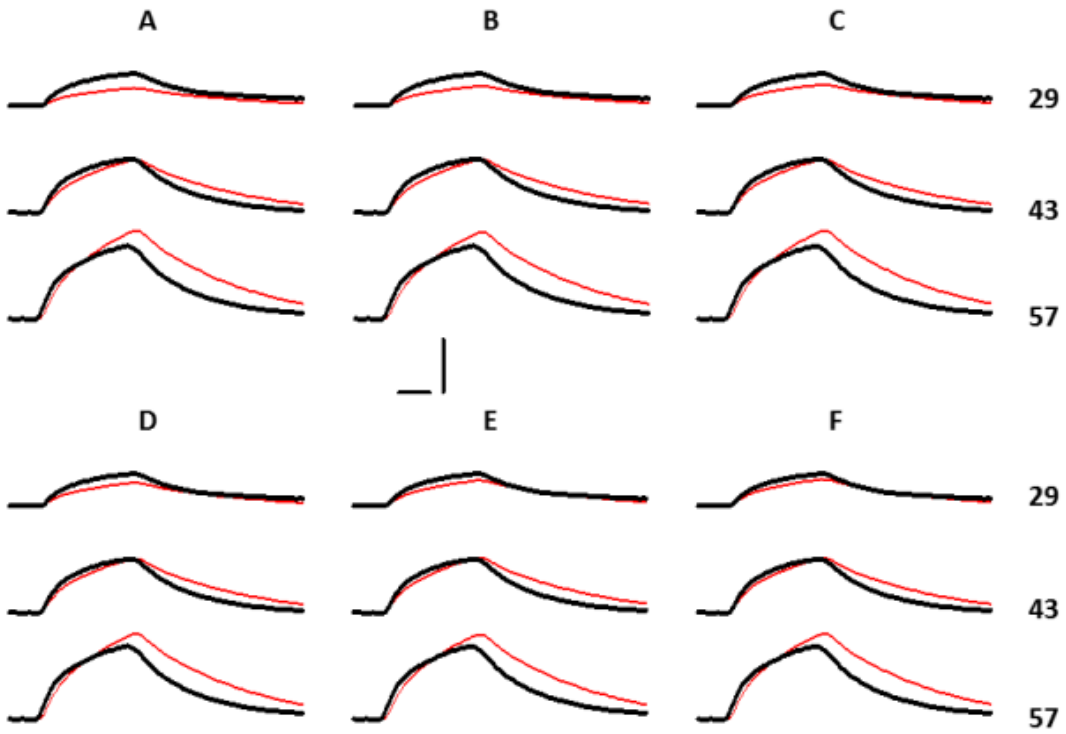

Fig. S3.3. Calibration of the model of MCs. In each part of the figure the real potentials experimentally measured in different retinal layers (black lines) are compared with the model simulations for the same depth (red lines). The retinal depth (in %) is marked on the right. Settings: *A* – sets o1-i1-m1; *B* – sets o1-i1-m2; *C* – sets o1-i1-m3; *D* – sets o2-i2-m1; *E* – sets o2-i2-m2; *F* – sets o2-i2-m3. Horizontal scaling mark – 1 s, vertical mark – 1 mV.

To better evaluate how close the model result was to reality, the potentials in more than one retinal layer should be compared. As we can see, the voltages calculated for 43% of the retinal depth (the middle row in each group) are almost identical to the real voltage with all 6 combinations of the settings that are shown in Fig. S3.3. Resemblance is not always as good for the voltages in other layers, particularly with set combination o1-i1-m1 (Fig. S3.3A). However, with settings o2-i2-m2 and o2-i2-m3 (Fig. S3.3, E and F, respectively) the results of the

computation are very close to the experimental data at all depths. To quantitatively evaluate the similarity, a measure analogous to standard deviation, *diff*, was used:

$$diff = \sqrt{((e1 - m1)^2 + (e2 - m2)^2 + (e3 - m3)^2)/3}\ ,$$

where e1, e2, and e3 are amplitudes of the real potentials at the end of light stimulation and at the retinal depths of 29, 43 and 57 %, respectively; m1, m2, and m3 are amplitudes of potentials computed by the model at the same time and at corresponding locations. The delayed maximum of the potentials computed on the base of K^+ measurements is probably because the RC time constant of the K^+-selective microelectrode is a bit larger than the time constant of MCs.

		Set m1	Set m2	Set m3
Set o1	Set i1	0.191 (19.0)	0.179 (24.0)	0.171 (18.3)
Set o2	Set i1	0.148 (22.3)	0.134 (28.0)	**0.130** (22.0)
Set o1	Set i2	0.176 (14.3)	0.167 (18.7)	0.160 (14.0)
Set o2	Set i2	0.139 (17.7)	**0.128** (23.0)	**0.124** (17.3)

Table S3.1. Summary of the model calibration. The mean of quantitative measure, *diff*, calculated for 12 different settings in 3 matrixes is presented. The mean of R_{inp} for the best fit in each setting is in parentheses. The best settings are bolded. More explanation in the text.

Two other profiles of light-induced $[K^+]_o$ changes in Co^{++}-treated retinae were recorded, and two other matrixes were created and tested with the computer program. In one case the best fit between experimental and computed voltage traces was also achieved with setting o2-i2, but in the other setting o1-i1 gave better results. So, for quantitative evaluation of the resemblance between the experimental and computational results for all 12 different combinations of resistance sets, the minimum values of *diff* and the associated R_{inp} were averaged from the three $[K^+]_o$ matrices and are summarized in Table S3.1. The table demonstrates that the smaller

variations of R_o in retinal synaptic and nuclear layers (set o2) produced a closer fit than the more drastic variations (set o1). Taking into account the higher resistivity of the cytoplasm compared to the extracellular fluid (set i2) also makes the model more accurate than just assuming the resistivities are the same (set i1). Among the sets of R_m, the uniform distribution (m1) produced the worst fit compared to both the morphometric-based (m2) and electrophysiology-based (m3) distributions, and with the latter it was possible to achieve slightly better results than with the former.

The calibration of the model demonstrates that the combination of resistance sets o2 for R_o, i2 for R_i and m3 for R_m with the mean R_{inp} = 17.3 MΩ produces computed results which fit best to the experimental data. However, the combination of o2 for R_o, i2 for R_i and m2 for R_m with the mean R_{inp} = 23 MΩ is almost equally good. The third best fit was found for the combination of o2-i1-m3 with mean R_{inp} = 22 MΩ. For computational evaluation of the ability of the MC to generate K^+-evoked transretinal potentials in the mouse retina those three settings (o2-i1-m3, o2-i2-m2 and o2-i2-m3) were used.

NEWMAN, E.A. (1987). Distribution of potassium conductance in mammalian Muller (glial) cells: a comparative study. *The Journal of neuroscience* **7,** 2423-2432.

REICHELT, W., MÜLLER, T., PASTOR, A., PANNICKE, T., ORKAND, P., KETTENMANN, H. & SCHNITZER, J. (1993). Patch-clamp recordings from Müller (glial) cell endfeet in the intact isolated retina and acutely isolated Müller cells of mouse and guinea-pig. *Neuroscience* **57,** 599-613.